Physica Scripta. Vol. T30, 14–23, 1990.

47

# Excitation of Large Amplitude Plasma Waves

Francis F. Chen

Electrical Engineering Department and Institute of Plasma and Fusion Research, University of California, Los Angeles, CA 90024-1594, U.S.A.

*Received May 22, 1989*

**Abstract**

The basic principles of various methods for exciting large amplitude electron plasma waves are reviewed, with particular emphasis on the methods that pertain to plasma accelerators. We also discuss methods for producing dense plasmas suitable for accommodating the large electric fields possible in plasma waves.

## 1. What is "large amplitude"?

By "large", one usually means an amplitude that is not insignificant compared with the *cold-plasma wavebreaking* limit. This amplitude, at which electron excursions from one wavelength overlap those from the adjacent ones, is the same as that calculated for the maximum possible density fluctuation; that is, for $n_1 = n_0$. By Poisson's equation, we find

$$\nabla \cdot \boldsymbol{E} = -4\pi e n_1, \qquad n_1 \approx n_0$$

$$\nabla^2 \phi \approx 4\pi e n_0, \qquad |e\phi| \approx \frac{4\pi n_0 e^2}{m}\frac{m}{k^2} = \frac{\omega_p^2}{c^2 k^2} mc^2.$$

The largest useful phase velocity $v_\phi = \omega/k$ is the velocity of light $c$, so that the maximum potential is given by

$$|e\phi_{max}| \approx mc^2 = 0.5\,\text{MeV}.$$

The corresponding electric field $\boldsymbol{E}$ is

$$|E_{max}| = |k\phi_{max}| = \frac{\omega_p}{ce} mc^2 = 0.94\sqrt{n_0}\ \text{V/cm}.$$

For instance, for $n_0 = 10^{18}\,\text{cm}^{-3}$, $|E| = 1\,\text{GeV/cm}$. This is about $10^3$ times what is possible in a vacuum. If we define the relative amplitude

$$\varepsilon \equiv \phi/\phi_{max} = e\phi/mc^2,$$

then "large amplitude" would mean $\varepsilon$ greater than about 10%.

## 2. Excitation methods

We shall discuss the following known or proposed methods for exciting large amplitude plasma waves:

1. Beat-wave excitation (with laser beams)
2. Wake-field excitation (with electron beams)
3. Laser wake-field excitation
4. Relativistic electron beam excitation
5. Stimulated Raman scattering

## 3. Properties of large amplitude plasma waves

For future reference, we first summarize without proof some of the known properties of large amplitude electron plasma waves.

### 3.1. *Nonlinear frequency shift*

McKinstrie and Forslund [1] and Mori [2] have shown that the *only* nonlinear frequency shift as plasma waves get large is that due to the relativistic mass increase of the oscillating electrons. Thus, $m \to \gamma m$ and

$$\omega_p^2 \to \omega_{p0}^2/\gamma,$$

where $\omega_{p0}$ refers to the rest mass and $\gamma$ is the relativistic factor corresponding to the mean electron velocity in the wave. Though other nonlinear effects can distort the wave, the fundamental frequency is unchanged because the electric force felt by each electron depends, at least in one-dimensional systems, only on the number of charges on each side of it, and not on their positions.

### 3.2. *Wavebreaking limit*

The cold-plasma wavebreaking limit given above is modified by both finite temperature and relativistic effects. Thermal motions decrease the limiting amplitude because electron orbits overlap more easily, while relativistic effects increase the limit because electrons move more sluggishly. The known results are as follows:

(a) $T_e = 0$, $\gamma = 1$: $eE_{max} = m\omega_p v_\phi$ (as above, but for $v_\phi = c$)

(b) $T_e > 0$, $\gamma = 1$: (Coffey [3])

$$\frac{eE_{max}}{m\omega_p v_\phi} = (1 - \tfrac{8}{3}\alpha_t^{-1/4} + 2\alpha_t^{1/2} - \tfrac{1}{3}\alpha_t)^{1/2},$$

where

$$\alpha_t \equiv 3KT_e/mv_\phi^2.$$

(c) $T_e = 0$, $\gamma > 1$: (Akhiezer and Polovin [4])

$$\frac{eE_{max}}{m\omega_p v_\phi} = \sqrt{2}\,(\gamma_\phi - 1)^{1/2}.$$

(d) $T_e > 0$, $\gamma_\phi \gg 1$: (Katsouleas and Mori [5])

$$\frac{eE_{max}}{m\omega_p v_\phi} = \alpha_t^{-1/4}\,[\ln(2\gamma_\phi^{1/2}\alpha_t^{1/4})]^{1/2}.$$

This result was calculated with a waterbag distribution for the electrons. In accelerator applications, the relativistic effect dominates. For instance, if $KT_e = 10\,\text{eV}$ and $\gamma_\phi = 100$, this formula gives $eE_{max}/m\omega_p c = 8.55$, a considerable improvement over the cold, non-relativistic case.

### 3.3. *Harmonic generation*

At large amplitudes, the correlation between electron velocity and position causes the $E$-field to steepen into a sawtooth shape. The corresponding density fluctuation is highly peaked, as shown in Fig. 1 for the case $n_1/n_0 = 0.45$.

The amplitude of the $m$th Fourier harmonic is proportional to the $m$th power of the fundamental amplitude. The

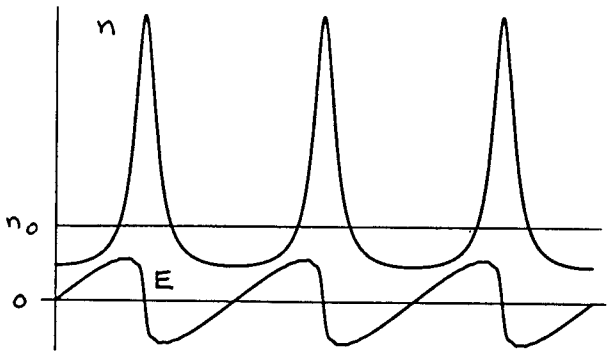


*Fig. 1.* Density and electric field waveforms for a nonlinear plasma wave with $n_1/n_0 = 0.45$.

coefficients for the cold-plasma case are given simply by Jackson [6]

$$\frac{n_m}{n_0} \approx \frac{m^m}{2^{m-1}m!}\left(\frac{n_1}{n_0}\right)^m.$$

## 4. Beat-wave excitation

This method utilizes two intense laser beams of slightly different frequencies, which beat in the plasma to form a fluctuating envelope, as illustrated in Fig. 2.

The ponderomotive force of this pattern bunches the electrons to excite a plasma wave, and the coupling is strong if the beat frequency is matched to the plasma wave frequency ($\approx \omega_p$).

### 4.1. *Phase matching*

Resonant coupling is obtained when the lasers' difference frequency and wavenumber ($\Delta\omega$, $\Delta\boldsymbol{k}$) are matched to those of the plasma wave ($\omega_p$, $\boldsymbol{k}_p$)

$$\omega_p = \omega_0 - \omega_2 \equiv \Delta\omega, \qquad \boldsymbol{k}_p = \boldsymbol{k}_0 - \boldsymbol{k}_2 \equiv \Delta k.$$

The two laser pump beams can be parallel, anti-parallel, or at an arbitrary angle. The last choice has advantages for the "Surfatron" accelerator, but that will not be discussed here. In parallel optical mixing, the $k$-matching condition results in a "fast" plasma wave with small $k_p$, as seen in Fig. 3(a). This is the case of interest for acceleration, since $v_\phi$ can be made arbitrarily close to $c$. The plasma wavelength is of order $\omega_p/c$, or about 100 $\mu$m for a typical $CO_2$ laser case. In anti-parallel mixing, it is seen from Fig. 3b that a "slow" plasma wave with large $k_p$ is generated. In underdense plasmas, it is clear that the plasma wavelength is then about half the laser wavelength, or $\approx 5\,\mu$m for $CO_2$ lasers.

### 4.2. *Group velocity matching*

Laser accelerators benefit from the fortunate synchronism between the group velocity $v_g$ of the laser pulse and the phase velocity of the plasma waves, and thus of the trapped particles. Since $\omega_p = \Delta\omega$ and $k_p = \Delta k$, we have

$$v_\phi = \frac{\omega_p}{k_p} = \frac{\Delta\omega}{\Delta k} \approx v_g.$$

Furthermore, since $v_g$ is given by

$$v_g = \left(1 - \frac{n}{n_c}\right)^{1/2} c, \quad \text{where} \quad \frac{n}{n_c} = \frac{\omega_p^2}{\omega_0^2}$$

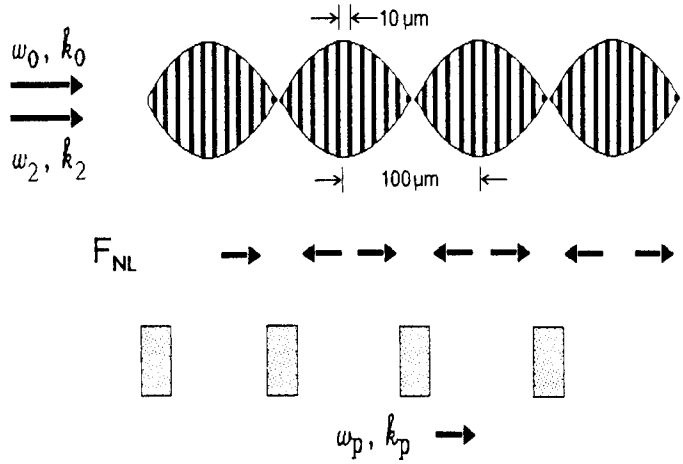


*Fig. 2.* Mechanism of beat-wave excitation.

and $v_\phi = v_g$, the $\gamma$-factor associated with $v_\phi$ is given by

$$\gamma_\phi \equiv \left(1 - \frac{v_\phi^2}{c^2}\right)^{-1/2} = \left[1 - \left(1 - \frac{n}{n_c}\right)\right]^{-1/2}$$
$$= \left(\frac{n_c}{n}\right)^{1/2} = \frac{\omega_0}{\omega_p}.$$

Thus, $\gamma_\phi$ is related to the plasma density simply by

$$\gamma_\phi = \omega_0/\omega_p.$$

### 4.3. *The Rosenbluth–Liu formula*

The higher the laser intensity, the faster the plasma wave will grow and the closer to the wavebreaking limit it will get. These relationships were derived by Rosenbluth and Liu [7] and can be recovered by the following simplified treatment using the electron fluid equations.

*Ponderomotive force*: The force on each cm$^3$ of fluid is (cf. Chen [8])

$$\boldsymbol{F}_{NL} = -\frac{\omega_p^2}{\omega_0\omega_2}\nabla\frac{\langle|\boldsymbol{E}_0 + \boldsymbol{E}_2|^2\rangle}{8\pi}.$$

We assume that $E_j$ varies as $\cos(k_j x - \omega_j t)$, where $j = 0, 2$, and that the time average of $E_j^2$ has no spatial gradient. The cross term $E_0E_2$ has the gradient $ik_p$, and we have

$$|F_{NL}| = \frac{\omega_p^2}{\omega_0\omega_2}k_p\frac{2E_0E_2}{8\pi}\tfrac{1}{2}[\cos(\omega_0 - \omega_2)t + \cos(\omega_0 + \omega_2)t]$$
$$= \frac{k_p}{2}\frac{n_0e^2}{m}\frac{E_0E_2}{\omega_0\omega_2}.$$

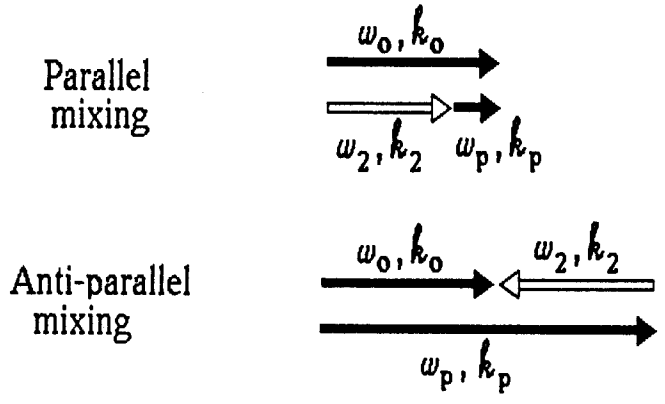


*Fig. 3.* Wavenumber matching for (a) parallel and (b) anti-parallel optical mixing.

Defining the laser field strength

$$\alpha \equiv \frac{v_{osc}}{c} = \frac{eE}{m\omega c},$$

we have for the ponderomotive force on each electron

$$f_{NL} = \tfrac{1}{2}k_p mc^2 \alpha_0 \alpha_2.$$

*Equation of motion*:

$$m\dot{v} = -eE + f_{NL}.$$

*Poisson's equation*:

$$\nabla \cdot \boldsymbol{E} = i\boldsymbol{k} \cdot \boldsymbol{E} = -4\pi e n_1.$$

*Equation of continuity*:

$$\ddot{n}_1 = -n_0 \nabla \cdot \dot{\boldsymbol{v}} = -ik_p \frac{n_0}{m}(-eE + f_{NL}).$$

Combining these equations, we obtain

$$\ddot{n}_1 = -\frac{4\pi n_0 e^2}{m} n_1 - ik_p \frac{n_0}{m}(\tfrac{1}{2}k_p mc^2 \alpha_0 \alpha_2)$$

$$= -\omega_p^2 n_1 - \tfrac{1}{2}ik_p^2 c^2 n_0 \alpha_0 \alpha_2.$$

If

$$n_1 = n_1(t) \exp(ik_p x - i\omega_p t),$$

then

$$\ddot{n}_1 \approx -2i\omega_p \dot{n}_1 - \omega_p^2 n_1,$$

so that

$$-2i\omega_p \dot{n}_1 = -\tfrac{1}{2}ik_p^2 c^2 n_0 \alpha_0 \alpha_2.$$

Since

$$k_p^2 c^2 \approx \omega_p^2,$$

we have

$$\dot{n}_1/n_0 = \tfrac{1}{4}\omega_p \alpha_0 \alpha_2.$$

Thus, the amplitude $\varepsilon$ grows linearly with time as

$$\varepsilon = \frac{n_1}{n_0} = \tfrac{1}{4}\alpha_0 \alpha_2 \omega_p t.$$

*Saturation.* As the waves grow, the electrons become more massive, and $\omega_p$ no longer matches the drivers' difference frequency $\Delta\omega$. This dephasing causes the growth to slow, stop, and then reverse. To calculate the maximum amplitude, we first evaluate the frequency shift $\delta\omega$

$$(\omega_p + \delta\omega)^2 = \omega_p^2/\gamma, \qquad \gamma = \left(1 - \frac{v^2}{c^2}\right)^{-1/2}$$

The equation of continuity yields

$$\varepsilon = \frac{n_1}{n_0} = \frac{k_p v}{\omega_p} = \frac{v}{v_\phi}, \qquad \frac{v^2}{c^2} = \frac{v_\phi^2}{c^2}\varepsilon^2.$$

Thus

$$\omega_p^2 + 2\omega_p \delta\omega \approx \omega_p^2\left(1 - \frac{1}{2}\frac{v_\phi^2}{c^2}\varepsilon^2\right),$$

$$\delta\omega \approx -\tfrac{1}{4}\omega_p \frac{v_\phi^2}{c^2}\varepsilon^2 \approx -\tfrac{1}{4}\omega_p \varepsilon^2(t).$$

The growth stops after a time $T$ when the phase has changed by $\pi/2$

$$\omega_p \int_0^T \tfrac{1}{4}\varepsilon^2(t)\,dt = \frac{\pi}{2}, \quad \text{where} \quad \varepsilon(t) \approx \tfrac{1}{4}\alpha_0 \alpha_2 \omega_p t.$$

Solving for $T$ and assuming that the linear growth rate holds up to that time, we obtain

$$\tfrac{1}{64}\omega_p^3 \alpha_0^2 \alpha_2^2 \int_0^T t^2\,dt = \frac{\pi}{2}, \qquad \tfrac{1}{3}\omega_p^3 T^3 = \frac{32\pi}{\alpha_0^2 \alpha_2^2},$$

$$\omega_p T = \left(\frac{96\pi}{\alpha_0^2 \alpha_2^2}\right)^{1/3}, \qquad \varepsilon_{sat} \approx \tfrac{1}{4}\alpha_0 \alpha_2 \omega_p T$$

$$\varepsilon_{sat} = \left(\frac{3\pi}{2}\alpha_0 \alpha_2\right)^{1/3} \propto I_0^{1/3}.$$

The standard result is only slightly different

$$\varepsilon_{sat} = (\tfrac{16}{3}\alpha_0 \alpha_2)^{1/3}.$$

The wave amplitude is seen to vary as the cube root of the laser intensity.

It would obviously be advantageous to adjust the density to a somewhat higher value so that the exact frequency match occurs not at the beginning but sometime during the growth of the wave. The optimum shift has been calculated by Tang *et al.* [9] whose results are shown in Fig. 4. A gain in $\varepsilon_{sat}$ of some 60% can be obtained this way, provided that other effects do not saturate the wave first.

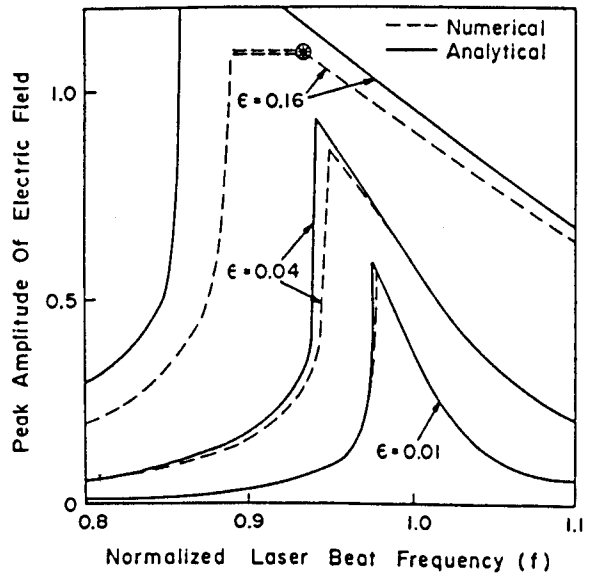


*Fig. 4.* Amplitude variation vs. normalized beat frequency $\Delta\omega/\omega_p$, for various pump strengths, showing the effect of detuning (Tang *et al.*, 1985).

### 4.4. *The beat-wave accelerator*

Large amplitude plasma waves can be used to accelerate electron or positron bunches which are injected into the wave troughs with velocities sufficiently close to $v_\phi$ to be trapped. How this could be done is illustrated in Fig. 5. A two-frequency laser pulse is seeded with electron bunches spaced by the plasma wavelength. With an intensity below the Raman threshold, no wave is excited except in the part of the plasma that has the resonant density. The plasma wave then grows around the bunches, trapping them. The trapping condition is approximately

$$\gamma > \frac{1 + \varepsilon^2}{2\varepsilon},$$

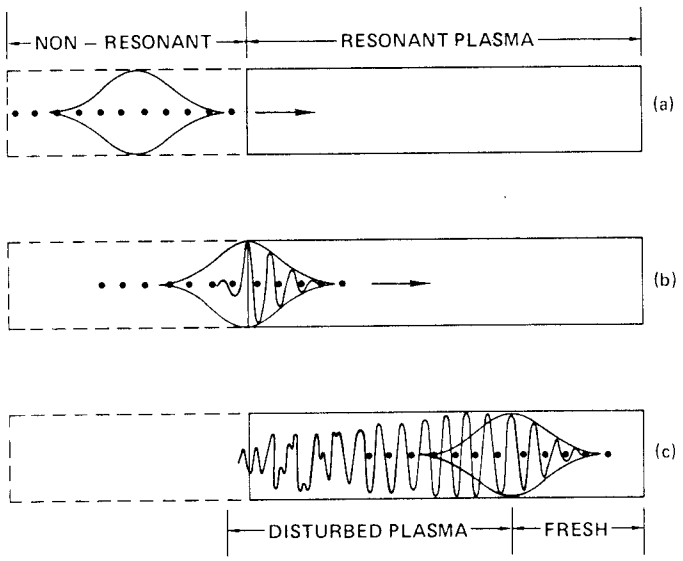


*Fig. 5.* Mechanism of particle injection and trapping in a beat-wave accelerator.

where $\gamma$ refers to the injection energy and $\varepsilon$ is the wave amplitude. The electrostatic field accelerates the electrons until they outrun the wave, at which time they must be ejected lest they enter a retarding field. This spatial dephasing limits the energy gain to

$$\Delta\omega \approx 4\varepsilon\gamma_\phi^2 mc^2.$$

Since the energy gained in each pass is limited, one can conceive of a staged accelerator (Fig. 6) in which each stage is adjusted with the proper density (and hence $\gamma_\phi$) to take advantage of the injection energy available from the last stage.

The electron bunches can be focused as well as accelerated when the plasma wave has a finite width. As shown in Fig. 7, the radial field of a two-dimensional wave can push the (positive) electrons toward the axis if the bunches are injected into the proper half of the half-cycle in which the longitudinal field is accelerating. If the wave is steepened, as shown in Fig. 1, it turns out that this 90° acceptance angle is increased for negative particles and decreased for positive ones.

## 5. Wake-field excitation

Large amplitude plasma waves can also be generated by an electron bunch from an existing accelerator. This wave can then be used to accelerate other bunches to even higher energy in the same way as discussed above. As shown in Fig. 8, a plasma-wave wake is excited behind an electron bunch because the cold electrons of the plasma are displaced by the fast-moving electrons of the bunch. When the bunch ends, it leaves behind a large positive charge imbalance, and

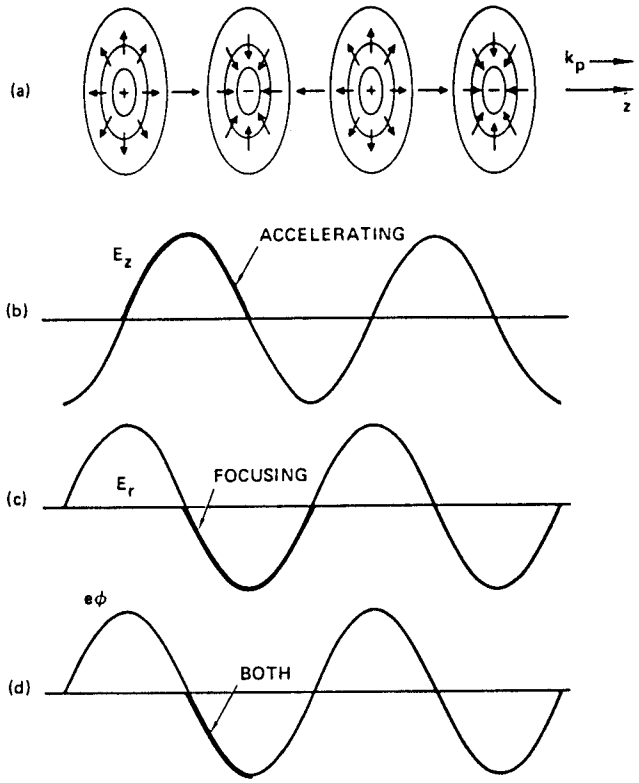


*Fig. 7.* Contours of constant electric potential in a two-dimensional plasma wave, showing the plasma region in which a positive particle must be injected in order to benefit from both the longitudinal and the radial electric fields.

the plasma electrons rush into neutralize it. The electrons overshoot and oscillate at the natural frequency of the plasma, which is $\omega_p$. Since the wave velocity must be the same as that of the bunch, or $\approx c$, the plasma wave has wave-number $k = \omega_p/c$, as in the beat-wave case.

The injected, accelerated bunch itself creates a wake; and if this wake is adjusted to be as large as the original wake and 180° out of phase with it, the wakes will cancel each other. The plasma wave energy is then completely transferred to the driven beam. The width of the wake cannot be smaller than the minimum size of a plasma wave, which is the skin depth $c/\omega_p$. This fact allows the driven beam to be made smaller than $c/\omega_p$ without sacrificing efficient energy transfer; thus, the driven particles need not sample the *radial* variation of field strength across the diameter of the wave. We now show how the energy spread due to the *axial* field variation can also be avoided by shaping the beam density.

*Green's function response.* Limiting the discussion to one-dimensional systems, we first compute the wake generated by a thin charge sheet $\sigma\delta(z)$ in the frame in which the sheet and the wake are stationary. The cold plasma then streams in with a velocity $\boldsymbol{u}$ (Fig. 9).

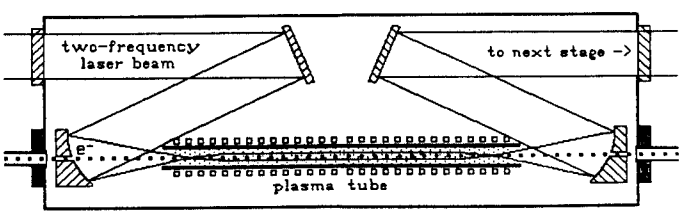


*Fig. 6.* A conceptual stage of a beat-wave accelerator.

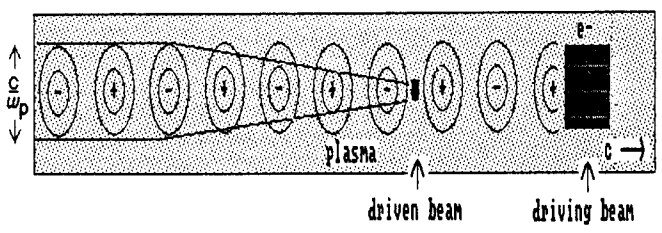


*Fig. 8.* Mechanism of wake-field excitation.

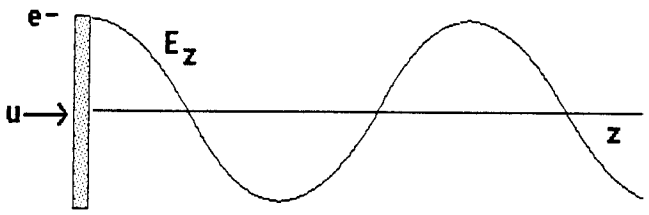


*Fig. 9.* The wake field of a sheet of electrons moving with velocity $\boldsymbol{u}$ to the left through a plasma, as seen in the moving frame.

The equations of motion, continuity, and Poisson give

$$m\boldsymbol{u}\cdot\nabla\boldsymbol{v} = -e\boldsymbol{E}, \qquad muv' = -eE$$

$$n_0\nabla\cdot\boldsymbol{v} + \boldsymbol{u}\cdot\nabla n_1 = 0, \qquad n_0 v' + un_1' = 0$$

$$\nabla\cdot\boldsymbol{E} = E' = 4\pi\sigma\delta(z) - 4\pi e n_1,$$

where $n_1$ is the fluctuating density of the plasma electrons, and $'$ stands for $\partial/\partial z$. Taking the space derivative and combining, we obtain

$$E'' = 4\pi\sigma\delta'(z) - 4\pi e n_1', \qquad n_1' = en_0E/mu^2$$

$$E'' + \frac{\omega_p^2}{u^2}E = 4\pi\sigma\delta'(z).$$

The solution is the Green's function response

$$E = 4\pi\sigma\cos k_p z \cdot U(z),$$

where $k_p = \omega_p/u$ and $U(z)$ is the step function $U(z) = \int\delta(z)\,dz$.

*Transformer ratio.* The wake from a beam of length $\boldsymbol{d}$ and charge density $\varrho(z)$ (Fig. 10) is found by integrating:

$$E(z) = 4\pi\int_0^z \varrho(z')\cos[k_p(z-z')]\,dz'.$$

We consider two density distributions $\varrho(z)$.

5.1. *Case of $\varrho(z) = \varrho_0 =$ constant*

$$E(z) = \frac{4\pi\varrho_0}{k_p}[\sin k_p(d-z) + \sin k_p z] \qquad z > d$$

$$= \frac{4\pi\varrho_0}{k_p}\sin k_p z \qquad z < d.$$

Let the beam be $N$ plasma wavelengths long, so that $k_p d = 2\pi N$. Then

$$E(z) = 2\sin k_p z \qquad z > d$$

$$= \sin k_p z \qquad z < d.$$

We define the *transformer ratio* to be the ratio between the largest accelerating field $E^+$ in the wake to the largest retarding field $E^-$ inside the beam

$$R \equiv |E^+/E^-|_{\max}.$$

We see that, in the case of constant $\varrho(z)$, $R$ is at most 2, indicating that an electron placed in the wake can be accelerated to at most twice the energy of the driving beam.

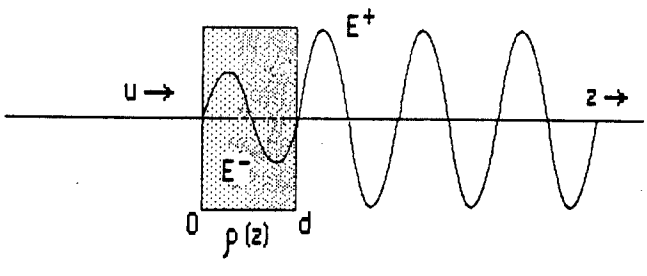


*Fig. 10.* The wake fields inside and behind a finite slab of electrons moving through a plasma.

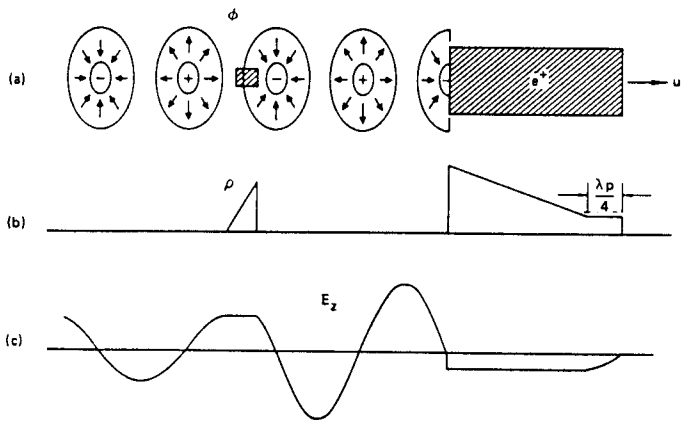


*Fig. 11.* Mechanism of the wake-field accelerator, showing (a) the relative positions of the driving and driven beams and the wake, (b) the ideal shapes of the beams, and (c) the uniform fields within the beams.

5.2. *Case of triangular bunch*

Now, suppose we let $\varrho = \varrho_0 k_p z$ for $0 \leqslant z \leqslant d$. Then integration of the Green's function yields

$$E_z = -\frac{4\pi\varrho_0}{k_p}2\pi N\sin k_p z \qquad z > d$$

$$= -\frac{4\pi\varrho_0}{k_p}(1-\cos k_p z) \qquad z < d$$

$$E_{\max}^+ = 2\pi N\left(\frac{4\pi\varrho_0}{k_p}\right), \qquad E_{\max}^- = 2\left(\frac{4\pi\varrho_0}{k_p}\right).$$

We see that the transformer ratio is improved by a factor $N$: $R = \pi N$. A further improvement can be obtained by removing the $\cos(k_p z)$ term inside the bunch ($z < d$). This can be done by adding a $\delta$-function precursor of the right magnitude to cancel that term [10]

$$\varrho(z) = \varrho_0 k_p z + 4\pi\sigma\delta(z) \quad \text{where} \quad \sigma = \varrho_0/k_p.$$

Integration then yields

$$E_z = \frac{4\pi\varrho_0}{k_p}(\cos k_p z - 2\pi N\sin k_p z) \qquad z > d$$

$$= \frac{4\pi\varrho_0}{k_p} = \text{constant} \qquad z < d.$$

The transformer ratio is now seen to be

$$R = [1 + (2\pi N)^2]^{1/2} \approx 2\pi N.$$

For instance, if $N = 16$, a 1-GeV driving beam can accelerate an injected beam to 100 GeV. The major benefit of the precursor is not the factor-2 increase in $R$ but in the creation of a *constant* retarding field inside the bunch. This means that each driving electron loses the same amount of energy, and the energy transfer to the plasma wave can be made to approach 100%. In practice, the $\delta$-function can be approximated by a "door step" precursor, as shown in the overall picture of the wake-field accelerator (Fig. 11).

The physical reason for the efficacy of the triangular shape is that the plasma electrons are displaced gradually but must rush back suddenly, thus causing a violent disturbance behind the pulse. The wake of the precursor causes a pre-acceleration of the driving electrons, allowing them to generate individual wakes of just the right phases to cancel the non-constant part of the $E$-field inside the bunch. Shaped electron bunches can be produced in the driving accelerator by the use of a photocathode illuminated by a shaped laser pulse. There is also a self-sharpening effect because the electrons in the rear of a non-ideal pulse feel a smaller retarding field and tend to move toward the front of the pulse. The relativistic mass increase of the plasma electrons in the wake also causes an apparent sharpening of the pulse because, as $\omega_p$ decreases, $k_p = \omega_p/c$ also decreases, and the plasma wavelength increases. Thus the pulse *seems* sharper on the scale of the plasma wave.

*Beam loading.* A short bunch of electrons can be efficiently accelerated by a wake field if injected at the point of maximum $E^+$. However, the energy spread will then be enormous because the electrons at the front of the bunch will feel only the wake of the driving bunch, while those at the rear will feel the wakes of both bunches. By shaping the injected bunch, the energy spread can be brought down to arbitrarily small values. Katsouleas *et al.* [11] have shown that the field inside an injected bunch can be made constant if it has a reverse triangular shape, as in Fig. 11. However, it must be injected at a point where $E^+$ is not maximum, and the wake is not completely cancelled. A compromise must be made among energy spread, accelerating field, and energy extraction efficiency. Figure 12 from Ref. 11 shows a computer simulation of a case where $E$ inside the bunch is $0.5E_{max}$, $E$ behind the bunch is also $0.5E_{max}$ so that the energy transfer is 75% efficient, and the energy spread is negligibly small.

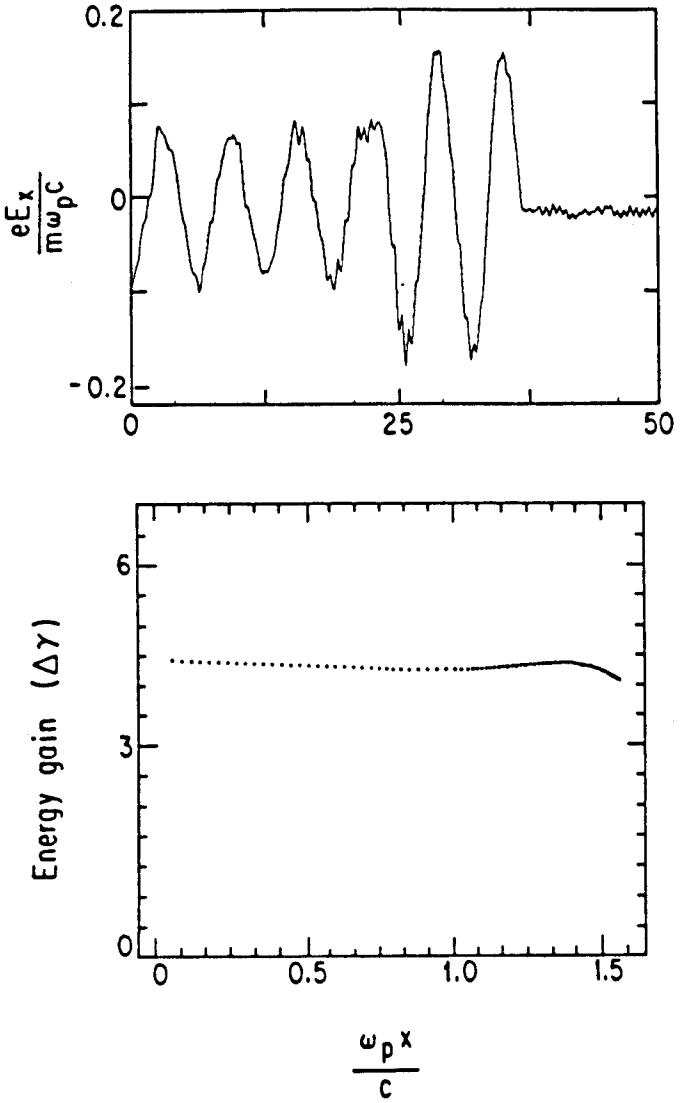


*Fig. 12.* Computer simulation of a properly loaded wake field, showing the uniformity of the field inside the driven beam and the resulting constancy of the energy gain by the electrons in the bunch. (Katsouleas *et al.*, 1987).

## 6. Laser wake-field excitation

Sprangle *et al.* [12] have pointed out that a wake field can be generated by an intense laser pulse as well as by an electron beam. This is shown schematically in Fig. 13. The ponderomotive force of the laser pulse envelope pushes electrons away both radially and axially. Upon returning, the electrons overshoot to form a region of excess negative charge. Subsequent oscillations must be at the frequency $\omega_p$, so a plasma wave is excited with $\omega_p/k_p$ equal to the group velocity of the laser pulse. As with ordinary wake-field excitation, the plasma density does not have to have a resonant value and for convenience can be made lower than the value of $\geqslant 10^{17}\,\mathrm{cm}^{-3}$ required in beat-wave excitation by the availability of laser line pairs.

One might ask why the plasma is needed, since the laser pulse's ponderomotive force can be used to accelerate particles directly. There are three reasons. First, the plasma brings the group velocity below the speed to light, to match the particle velocity. Second, the ponderomotive force on relativistic particles is lowered by the factor $\gamma$, and so it acts more strongly on the plasma electrons. Once the energy has been transferred to the wake, as we have seen, it can be extracted efficiently by proper loading. Third, a laser beam in vacuum would diffract, but a plasma can prevent this by the well-known phenomenon of relativistic self-focusing if the beam power is above the threshold of 17 $(\omega_0/\omega_p)^2$ GW (independent of spot size). The focusing is caused by the increase of the dielectric constant $1 - \omega_p^2/\omega^2$ near the axis, where the beam is most intense and the electrons have the largest $\gamma$-factor.

## 7. Stimulated Raman scattering

Plasma waves are often excited, unintentionally, by intense laser light through the phenomenon of stimulated Raman

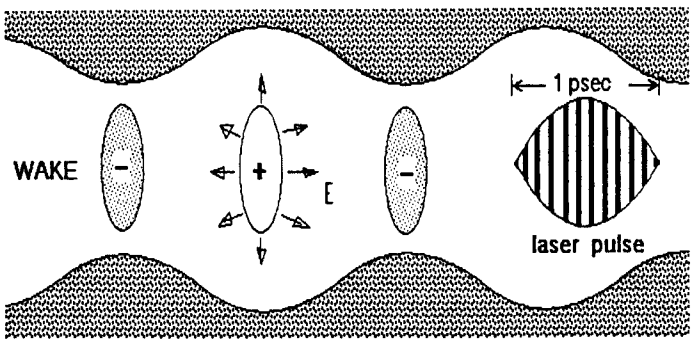


*Fig. 13.* Mechanism of the laser wake-field accelerator.

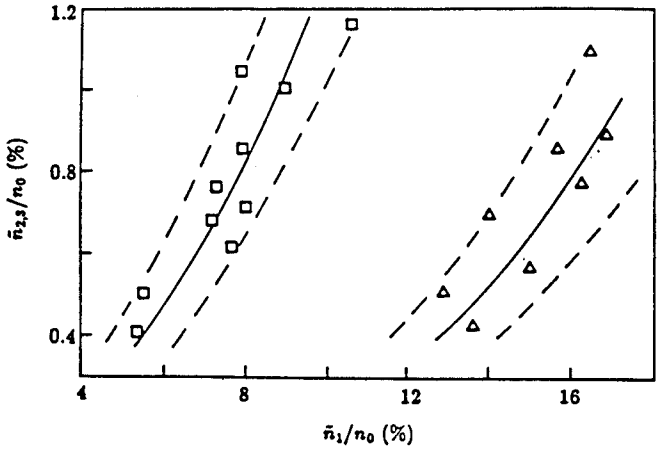


*Fig. 14.* Measured amplitudes of the 2nd ($n_2$) and 3rd ($n_3$) harmonics of $\omega_p$ in a nonlinear of plasma wave, vs. the fundamental amplitude. (Umstadter *et al.*, 1987).

scattering (SRS). In this instability, a pump beam ($\omega_0$, $\boldsymbol{k}_0$) is reflected from an underdense plasma by a plasma wave ($\omega_p$, $\boldsymbol{k}_p$), which itself is excited by the beat between the pump and the reflected wave ($\omega_2$, $\boldsymbol{k}_2$). The diagrams for Fig. 3 can be used for forward and backward SRS if we understand that ($\omega_2$, $\boldsymbol{k}_2$) is now a daughter wave rather than a pump. SRS forward scatter would generate plasma waves fast enough to be of interest for accelerators, but SRS backscatter has the lower threshold. Compared with beat-wave excitation, SRS has the advantages that only one pump frequency is needed, and the density need not be resonant. Disadvantages are that the phase of the plasma wave is not controllable, and much higher intensities are required.

High intensity brings in a number of disastrous competing effects, mostly stemming from stimulated Brillouin scattering (SBS), which usually has a lower threshold than SRS. The ion wave created by SBS causes a density ripple, and thus a non-uniform value of $\omega_p$. On the one hand, this can cause mode coupling to other wavelengths, as predicted by Barr and Chen [13]; on the other, it can suppress the fundamental, as observed by Walsh *et al.* [14]. SBS effects have also been observed in beat-wave excitation [15], where SBS-reflected light forms a pair of counter-propagating pumps and leads to extensive mode coupling.

SRS backscatter has been used successfully, however, for the study of nonlinear plasma waves by Umstadter *et al.* [16] Their measurements of harmonic generation (Fig. 14) are seen to agree with the theoretical formula given earlier in this paper.

## 8. Relativistic electron beam excitation

The first experiments on plasma waves employed low-current electron beams for their excitation. With the power available now from diode sources of relativistic electron beams (REBs), one might hope that much larger amplitude waves can be generated by REBs. The scheme proposed by Nation *et al.* [17] is shown in Fig. 15, and the corresponding ($\omega$, $k$) diagram in Fig. 16.

The REB of velocity $\boldsymbol{v}_0$ is guided by a uniform magnetic field and passes through a magnetic wiggler of wave number $k_0$. Four space-charge waves are possible on the beam: a plasma wave and a cyclotron wave going in each direction

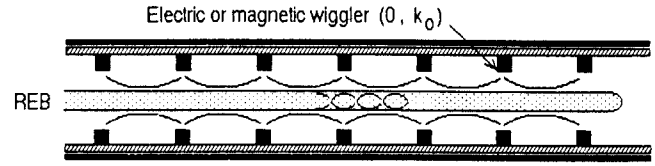


*Fig. 15.* Schematic of plasma wave excitation on a relativistic electron beam in a stationary wiggler.

relative to $\boldsymbol{v}_0$. The forward-propagating "fast" waves have positive energy, while the backward propagating "slow" waves have negative energy. A fast wave and a slow wave can be excited simultaneously without net change of energy if they can be coupled together by the "pump", which in this case is the stationary wiggler ($\omega_0$, $k_0$). Since $\omega_0 = 0$, the excited waves have $\omega_2 = \omega_1 + \omega_0 = \omega_1$, as shown by the horizontal line in Fig. 16. The $\boldsymbol{k}$ of the wiggler is then adjusted so that $\boldsymbol{k}_2 = \boldsymbol{k}_1 = \boldsymbol{k}_0$. In this manner, the fast and slow plasma waves have been successfully excited.

For accelerator purposes, however, the fast plasma wave is not close enough to the velocity of light, and one has to excite the fast cyclotron wave, which can cross the light line. Though in principle possible, this has not yet been accomplished.

## 9. Plasma sources for accelerators

### 9.1. *Requirements*

Excitation of large amplitude plasma waves requires a suitable source of plasma. Accelerator applications impose severe requirements on the plasma generators; some are listed below.

1. High density: $10^{14}$–$10^{18}\,\mathrm{cm}^{-3}$
2. High aspect ratio: 10–100 cm long, 1–10 mm in diameter
3. Quiescent
4. Constant or reproducible density.
5. Density uniform longitudinally (or with controllable gradient)

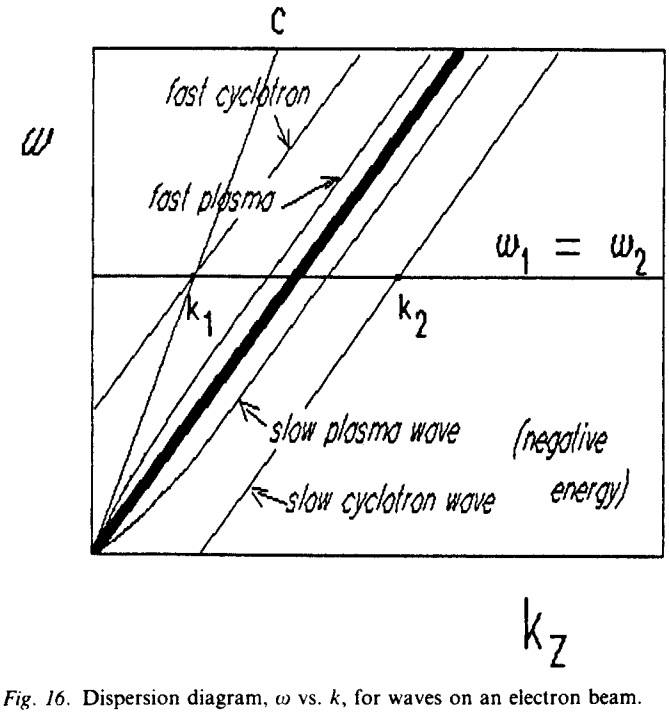


*Fig. 16.* Dispersion diagram, $\omega$ vs. $k$, for waves on an electron beam.

6. Density uniform radially (or with controllable reverse gradient)
7. Fully ionized (low $Z$)
8. Heavy ions (high $Z$)
9. Zero or small magnetic field (or controllable transverse field for the Surfatron)
10. Beam access along the axis
11. Simple, cheap, rugged, and dependable
12. Efficient, with simple power supplies

It is clear that some of these requirements are conflicting.

High density is dictated by $E_{max} \propto \sqrt{n}$ and by laser beat frequencies. The length must match the acceleration length. Quiescence, reproducibility, and uniformity are required to keep $\omega_p$ fixed. The allowable tolerance can be estimated from the maximum frequency shift due to relativistic effects; namely, $|\delta\omega| \approx \frac{1}{4}\varepsilon^2\omega_p$, as we saw previously. Keeping $\delta\omega_p < \delta\omega$, we have

$$\frac{\delta\omega_p}{\omega_p} = \frac{1}{2}\frac{\delta n}{n} < \tfrac{1}{4}\varepsilon^2.$$

Thus, $\delta n/n < \frac{1}{2}\varepsilon^2$, or about 1% for a 10% wave.

Fully stripped, low-$Z$ ions are preferred for use with intense lasers, since further ionization by the laser beam can change the density unless there is not enough time. On the other hand, heavy ions are preferred in order to increase the time available before instabilities, such as SBS, which involve ion motion, can develop. Strong magnetic fields are generally incompatible with electron beam focussing and should be avoided. Discharges requiring electrodes across the axis are similarly unsuitable. The last two requirements are obviously desirable for multi-staged accelerators pulsed repetitively for long periods.

### 9.2. *Possible sources*

We discuss below eleven possible ways to produce high-density plasmas in which one could generate large electric fields in plasma waves. Diagrams are omitted to save space, but references are given from which the reader can obtain further information and other references.

1. *High current arcs.* A simple capacitor discharge between two tungsten or molybdenum electrodes has been used in many experiments on laser-plasma interactions. With voltages of a few kilovolts, the electrodes may be 1–20 cm apart and be plane, curved, needle-pointed, or cylindrical (for axial beam access). No magnetic field is necessary. Properties of a hollow-electrode arc were studied by Turechek and Chen [18]. With pressures of 1–10 torr of H, He, or A, densities of order $6 \times 10^{16}\,\mathrm{cm}^{-3}$ were created with $T_e$ of a few eV and about 10% ionization. Laser heating with a $CO_2$ beam raised the density to above $5 \times 10^{17}\,\mathrm{cm}^{-3}$ at 100% ionization, with temperatures of 30–100 eV, depending on the $Z$ of the gas. The uniformity of the laser-heated region has been verified by Herbst *et al.* [19], and a smaller version of this discharge was used successfully to demonstrate beat-wave excitation [20]. Reproducibility is greatly improved over laser breakdown of a neutral gas. A variation called a hollow-cathode arc has been used by Rosenzweig [21] for experiments on wake-field acceleration. This is a low-voltage discharge ($\approx 100$ V) with a ring anode and a large tubular cathode which heats up to electron emission. Disadvantages of the arc method are the lack of full ionization and the high $T_e/T_i$ ratio, which permits the SBS threshold to be low.

2. *Theta pinch.* Large theta pinches have been used extensively in magnetic fusion and X-ray source work, but small ones tailored for high density (up to $10^{18}\,\mathrm{cm}^{-3}$) and low temperature are useful sources for large amplitude wave excitation. There is good access along the axis; the plasma is fully ionized; and the $T_e/T_i$ temperature ratio is $\leqslant 1$, so that ion fluctuations are suppressed by Landau damping. Amini and Chen [22, 23] have measured a pinch with a 10 cm diameter, 20 cm long coil and a 30 kV, 6 kJ capacitor bank and used it for experiments on anti-parallel beat-wave excitation and Raman scattering at $6 \times 10^{16}\,\mathrm{cm}^{-3}$ density. For electron acceleration work, however, theta pinches suffer from their strong magnetic field, which interferes with the electron optics of the injected beam [24]. Though the axial magnetic field of the pinch should be straight near the axis, irregularities of the high-beta plasma have been found to distort the field [25].

3. *Z-pinch.* Though these are in principle unstable, the period of stability is much longer than required for experiments on electron acceleration. Handke *et al.* [26] have successfully used $z$-pinches up to $2 \times 10^{18}\,\mathrm{cm}^{-3}$ density for SBS experiments. There is no reason why the electrodes could not have a central hole for beam access, but the plasma is again high-beta, so that irregular magnetic fields can be expected.

4. *Laser ionization of gases.* Early experiments requiring long-scalength plasmas utilized high-current solenoids to generate magnetic fields of order 100 kG in order to confine plasmas ionized by a $CO_2$ laser beam [27, 28]. Experiments on SBS were done up to densities of order $2 \times 10^{18}\,\mathrm{cm}^{-3}$. For accelerator purposes, however, the density scalelength may not be long enough; the strong magnetic field would interfere with electron focussing; and the method is rather complicated and expensive. Since the photon energy for $CO_2$ light is only 0.12 eV, it requires about 100 photons to ionize an atom. The physical processes here are simply the collisional absorption of the laser energy and avalanche ionization by the heated electrons.

Smaller plasmas, with scalelengths of order 100 $\mu$m, can be created without magnetic confinement by laser ionization of a gas jet (see, for instance, [29]). These plasmas are usually created at high density and allowed to decay and spread before being used. A recent study of $CO_2$–laser ionization of puffs from a fast gas valve by Martin *et al.* [30] showed that full ionization occurs in less than 1 nsec, much faster than in collisional ionization. The authors postulate that Keldysh tunneling ionization dominates in the early stages and collisional ionization occurs at later times. Using laser intensities in the $2\text{–}4 \times 10^{14}\,\mathrm{W/cm}^2$ range, they achieve densities of $10^{17}\text{–}10^{18}\,\mathrm{cm}^{-3}$ in a 1-mm sized plasma at $N_2$ pressures of 0.3–2 torr, ionized to $Z \approx 3$.

5. *Multi-photon ionization.* Nd-glass lasers operating at 1.06 or 0.53 $\mu$m have photon energies up to 2.3 eV and hence can ionize an atom with only 6 photons. Dangor *et al.* [31] have studied this process with a 10 J, 100 ps, frequency-doubled glass laser focussed to $10^{14}\,\mathrm{W/cm}^2$. Complete ionization of 0.5–4 torr of $H_2$ was achieved in a time much shorter than a collision time, giving an 8–10 eV plasma uniform to 4% over 8 mm. The radial uniformity was not measured; but since multi-photon ionization is complete once a threshold

intensity is exceeded, it was expected that the plasma was at least initially uniform radially. This has proved to be a very convenient plasma production method, but a large laser is needed, the uniform plasma is rather small in diameter and length, and the density changes fast since there is no confinement.

6. *Laser ionization of solid targets.* The blow off plasma from a flat, solid target has traditionally been used in experiments relevant to laser fusion. The technique has not been refined so that predictably long scalelengths can be obtained. To avoid a critical-density layer in the path of the laser beam, Bernard *et al.* [32] have used the edge of a carbon disk, and Figueroa *et al.* [33] have developed thin plastic film targets giving a controllable value of the maximum density. The Osaka group has proposed a plasma-fibre accelerator [34] in which laser light impinging on the inside of a hollow tube creates a plasma with an inverse (and hence focussing) density gradient.

7. *ECRH sources.* Production of plasmas by electron cyclotron resonance (ECRH) is commonly used in fusion and plasma processing machines. Though these plasmas may be useful for experiments using microwave or far-infrared pumps, the densities are rather small and the size unnecessarily large for use in laser accelerators. The microwave-oven frequency of 2.45 GHz is almost universally used; the corresponding magnetic field is 875 G. Typical densities are $\leqslant 10^{2}\,\mathrm{cm}^{-3}$ at microwave powers of $\leqslant 1$ kW [35]. Plasma confinement can be improved by lining the walls of the chamber with permanent magnets, forming a magnetic bucket [36]. The density can be increased by a brute-force increase in power. Experiments with an external helical antenna [37] with 10–100 kW of power showed that $n = 2 \times 10^{13}\,\mathrm{cm}^{-3}$ at 20 kW and $9 \times 10^{13}\,\mathrm{cm}^{-3}$ at 90 kW, with $T_e \approx 2$ eV and $\approx 80\%$ ionization. With high-power microwave sources the main problem is breakdown in the waveguide at the vacuum window and wherever the field is near 875 G. The frequency of 2.45 GHz is below the plasma frequency for all densities above $7.45 \times 10^{10}\,\mathrm{cm}^{-3}$, so that plasma waves excited in such devices may have a low-frequency modulation.

8. *Radiofrequency (RF) sources.* A more efficient way to generate densities in the $10^{13}$–$10^{14}\,\mathrm{cm}^{-3}$ range is the helicon-wave source developed by Boswell [38]. This source employs a dc magnetic field of $\leqslant 1$ kG and an external antenna. There is complete access along the axis. Using 1 kW of the power at 7 MHz, Boswell obtained a peak density of $10^{13}\,\mathrm{cm}^{-3}$ in a 5 cm diameter, 100 cm long tube; and the argon plasma appeared to be completely ionized along the axis. Using higher power, the density has reached $10^{14}\,\mathrm{cm}^{-3}$. Chen [39] has explained the efficiency of ionization by the trapping and acceleration of plasma electrons by the helicon wave. Experiments at 31 MHz have shown that the optimum wave velocity is that which brings the electrons to the optimum energy for ionization. Power supplies are readily available at the industrial standard frequencies of 13.56 and 27.12 MHz.

9. *Ultraviolet (UV) ionization.* That UV radiation is readily absorbed in ionizing a gas has been known for many years, and this fact has been used in early TEA $CO_2$ lasers. It has been proposed (J. M. Dawson, private communication) to use glass-laser flashlamps to produce a long, slender column of plasma for accelerator purposes. Flashlamp tubes are available which transmit down to 170 nm, which corresponds to 7.2 eV photons. A gas like Xe, which as a large cross section and a threshold of 12.13 eV, could possibly be ionized efficiently by UV. Only partial ionization can be expected, however.

10. *Capillary discharges.* To produce densities above the $10^{17}\,\mathrm{cm}^{-3}$ range, one could use capillary discharges, which were discovered in the USSR and recently used by Zigler [40]. Two electrodes are separated by a plastic insulator with a capillary hole or slit. A 60 $\mu$F, 2 kV capacitor is discharged through the slit in vacuum, and a puff of gas (mostly CH) is driven through a slit in the anode. This puff can then be ionized with a small laser, forming a plasma of density $10^{19}$–$10^{21}\,\mathrm{cm}^{-3}$, which can then be allowed to decay to the desired density.

11. *Quasi-resonant laser ionization.* Alkali metals vaporized in a heat pipe can be ionized to densities of order $10^{16}\,\mathrm{cm}^{-3}$ with a small (0.2 J) laser [41]. The mechanism for the efficient ionization is only now being understood. Using a 2 J, 2 $\mu$sec dye laser at 589 n, tuned to the sodium D-line doublet, Bardet *et al.* [42] have recently produced a density of $6 \times 10^{16}\,\mathrm{cm}^{-3}$ at $T_e < 1$ eV. If axial uniformity can be achieved, this method could possibly be developed into an interesting accelerator source 10–20 cm long.

## Acknowledgment

This work was supported by the National Science Foundation, Grant ECS 87-12089.

## References

1. McKinstrie, C. J. and Forslund, D. W., Phys. Fluids **30**, 904 (1987).
2. Mori, W. B., IEEE Transactions on Plasma Science **PS-15**, 88 (1987).
3. Coffey, T. P., Phys. Fluids **14**, 1402 (1971).
4. Akhiezer, A. I. and Polovin, R. V., Sov. Phys. JETP **3**, 696 (1956).
5. Katsouleas, T. and Mori, W. B., Phys. Rev. Lett. **61**, 90 (1988).
6. Jackson, E. A., Phys. Fluids **3**, 831 (1960).
7. Rosenbluth, M. N. and Liu, C. S., Phys. Rev. Lett. **29**, 701 (1972).
8. Chen, F. F., Introduction to Plasma Physics and Controlled Fusion, 2nd ed., Vol. 1, p. 305ff (1984).
9. Tang, C. M., Sprangle, P. and Sudan, R. N., Phys. Fluids **28**, 1974 (1985).
10. Chen, P., Su, J. J., Dawson, J. M., Bane, K. L. F. and Wilson, P. B., Phys. Rev. Lett. **56**, 1252 (1986).
11. Katsouleas, T., Wilks, S., Chen, P., Dawson, J. M. and Su, J. J., Particle Accelerators **22**, 81 (1987).
12. Sprangle, P., Esarey, E., Ting, A. and Joyce, G., Appl. Phys. Lett. **53**, 2146 (1988).
13. Barr, H. C. and Chen, F. F., Phys. Fluids **30**, 1180 (1987).
14. Walsh, C. J., Villeneuve, D. M. and Baldis, H. A., Phys. Rev. Lett. **53**, 1445 (1984).
15. Darrow, C., Umstadter, D., Katsouleas, T., Mori, W. B., Clayton, C. E. and Joshi, C., Phys. Rev. Lett. **56**, 2629 (1986).
16. Umstadter, D., Williams, R., Clayton, C. E. and Joshi, C., Phys. Rev. Lett. **59**, 292 (1987).
17. Nation, J. A., Anselmo, A. and Greenwald, S., in New Developments in Particle Acceleration Techniques (Edited by S. Turner), CERN publication 87-11, **II**, 623 (1987).
18. Turechek, J. J. and Chen, F. F., Phys. Fluids **24**, 1126 (1981).
19. Herbst, M. J., Clayton, C. E. and Chen, F. F., J. Appl. Phys. **51**, 4080 (1980).
20. Clayton, C. E., Joshi, C., Darrow, C. and Umstadter, D., Phys. Rev. Lett. **54**, 2343 (1985).
21. Rosenzweig, J. B., Cole, B., Gai, W., Koneckny, R., Norem, J., Schoessow, P., and Simpson, J., in Conf. Proceedings Vol. 193: Advanced Accelerator Concepts, p. 340. Amer. Inst. Phys., New York (1989).
22. Amini, B. and Chen, F. F., Phys. Rev. Lett. **53**, 1441 (1984).

23. Amini, B. and Chen, F. F., Phys. Fluids **29**, 3864 (1986).
24. Joshi, C., Clayton, C., Marsh, K., Williams, R. and Leemans, W., in New Developments in Particle Acceleration Techniques (Edited by S. Turner), CERN Publication 87-11, **II**, 351 (1987).
25. Leemans, W. P., Clayton, C. E. and Joshi, C., Rev. Sci. Instrum. **59**, 1641 (1988).
26. Handke, J., Rizvi, S. A. H. and Kronast, B., Phys. Rev. Lett. **51**, 1660 (1983).
27. Offenberger, A. A., Cervenan, M. R., Yam, A. M. and Pasternak, A. W., J. Appl. Phys. **47**, 1451 (1976).
28. Massey, R., Berggren, K. and Pietrzyk, Z. A., Phys. Rev. Lett. **36**, 963 (1976).
29. Al-Shiraida, Y. S., Offenberger, A. A. and Rozmus, W., Phys. Rev. Lett. **52**, 283 (1984).
30. Martin, F., Brodeur, P., Matte, J. P., Pepin, H. and Ebrahim, N., Conf. Proceedings Vol. 156: Advanced Accelerator Concepts, p. 121. Amer. Inst. Phys., New York (1987).
31. Dangor, A. E., Dymoke-Bradshaw, A. K. L., Dyson, A., Garvey, T., Mitchell, I., Cole, A. J., Danson, C. N., Edwards, C. B. and Evans, R. G., Conf. Proceedings Vol. 156: Advanced Accelerator Concepts, p. 112. Amer. Inst. Phys., New York (1987).
32. Bernard, J. E., Baldis, H. A., Villeneuve, D. M. and Estabrook, K., Phys. Fluids **30**, 3616 (1987).
33. Figueroa, H., Joshi, C., Clayton, C. E., Azechi, H., Ebrahim, N. A. and Estabrook, K., in Laser Interaction and Related Plasma Phenomena (Edited by H. Hora and G. M. Miley), Vol. 6, 527 (1984).
34. Barnes, D. C., Kurki-Suonio, T. and Tajima, T., IEEE Trans. on Plasma Sci. **PS-15**, 154 (1987).
35. Popov, G. A., J. Vac. Sci. Technol. **A7**, 894 (1989).
36. Asmussen, J., J. Vac. Sci. Technol. **A7**, 883 (1989).
37. Petty, C. C. and Smith, D. K., Rev. Sci. Instrum. **57**, 2409 (1986).
38. Boswell, R. W., Plasma Physics and Controlled Fusion **26**, 1147 (1984).
39. Chen, F. F., Laser and Particle Beams **7**, 551 (1989).
40. Zigler, A., Lee, R. W., and Mrowka, S., Laser and Particle Beams **7**, 369 (1989).
41. Lucaturto, T. B. and McIlrath, T. J., Phys. Rev. Lett. **37**, 428 (1976).
42. Bardet, J. P., Bobin, J. L., Dimarcq, C., Giry, L., Larour, J. B., Valognes, J. C. and Zaibi, M. A., Laser and Particle Beams (to be published) (1989).